

Electric-Field-Induced Conductance Switching in FeCo Prussian Blue Analogues

Osamu Sato,^{*,†} Tomoko Kawakami,^{†,‡} Masanobu Kimura,[†] Shoko Hishiya,[†] Shoichi Kubo,[†] and Yasuaki Einaga[‡]

Kanagawa Academy of Science and Technology, KSP Building, East 412, 3-2-1 Sakado, Takatsu-ku, Kawasaki-shi, Kanagawa 213-0012, Japan, and Department of Chemistry, Faculty of Science and Technology, Keio University, 3-14-1 Hiyoshi, Yokohama 223-8522, Japan

Received June 21, 2004; E-mail: sato@photo-science.jp

One of the main challenges in molecular materials science is the design of compounds exhibiting multiple physical properties. Several examples of such compounds have recently been reported.¹ These include a molecular metal with ion-conducting channels,^{1a} a molecule-based layered compound with ferromagnetism and metallic conductivity,^{1b} and so on. Furthermore, to apply these materials, it is desirable to be able to control their physical properties by some external stimuli. Prussian blue analogues are promising compounds for such a purpose. It has been reported that their color can be reversibly switched by electrochemical treatments.² Furthermore, they have recently attracted attention as tunable molecular magnets as well as high T_c magnets.^{3,4} This means that their optical and magnetic properties can be controlled by some external perturbations. However, although many studies have been performed on their transport properties,⁵ there have been no reports as yet of drastic changes in their conductivity.⁶ Here, we describe electric-field-induced conductance transitions as well as thermally induced conductivity switching observed in FeCo Prussian blue analogues. This finding shows that not only magnetic and optical properties but also conducting properties can be switched by external perturbations in FeCo Prussian blue analogues.

Three kinds of FeCo Prussian blue were prepared via a simple solution-mixing method.⁷ These were $\text{Na}_{0.5}\text{Co}^{\text{II}}_{1.25}[\text{Fe}^{\text{III}}(\text{CN})_6] \cdot 4.8\text{H}_2\text{O}$, $\text{Na}_{0.38}\text{Co}^{\text{II}}_{1.31}[\text{Fe}^{\text{III}}(\text{CN})_6] \cdot 5.4\text{H}_2\text{O}$, and $\text{Rb}_{0.5}\text{Co}^{\text{III}}\text{Co}^{\text{II}}_{0.25}[\text{Fe}^{\text{II}}(\text{CN})_6] \cdot 5.9\text{H}_2\text{O}$, which are hereafter designated as compounds **1**, **2**, and **3**, respectively.⁷ Their powder X-ray diffraction patterns were consistent with a face-centered cubic structure. The unit cell parameters for **1**, **2**, and **3** were 10.27, 10.24, and 10.02 Å, respectively. IR spectra measured at room temperature showed that CN stretching peaks were observed at ca. 2160, 2160, and 2120 cm^{-1} for **1**, **2**, and **3**, respectively. This means that the main components of **1**, **2**, and **3** at room temperature are the $\text{Fe}^{\text{III}}\text{-LS-CN-Co}^{\text{II}}\text{-HS}$, $\text{Fe}^{\text{III}}\text{-LS-CN-Co}^{\text{II}}\text{-HS}$, and $\text{Fe}^{\text{II}}\text{-LS-CN-Co}^{\text{III}}\text{-LS}$ moieties, respectively.⁴ The magnetic properties were measured under a DC magnetic field of 5000 G. The products of molar magnetic susceptibility (χ_M) and temperature for compounds **1–3** are shown as a function of temperature (Figures 1 and 2). The $\chi_M T$ values for **1** and **2** varied significantly, depending on temperature, because of the phase transition between the $\text{Fe}^{\text{III}}\text{-LS-CN-Co}^{\text{II}}\text{-HS}$ states and the $\text{Fe}^{\text{II}}\text{-LS-CN-Co}^{\text{III}}\text{-LS}$ states. The phase-transition temperatures of **1** in cooling and heating modes are $T_{1/2}^{\downarrow} = 248$ K and $T_{1/2}^{\uparrow} = 275$ K, respectively. $T_{1/2}^{\downarrow}$ is the temperature where, in the cooling mode, there is 50% of the high-temperature phase, and $T_{1/2}^{\uparrow}$ is the temperature where, in the heating mode, there is 50% of the low-temperature phase. The phase transition temperatures of **2** are $T_{1/2}^{\downarrow} = 213$ K and $T_{1/2}^{\uparrow} = 235$ K, respectively. In contrast,

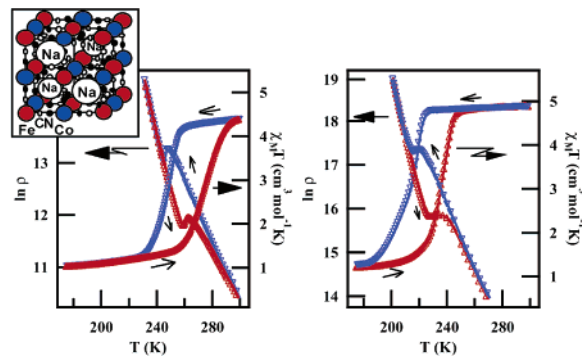


Figure 1. Temperature dependence of resistivity and magnetization for compounds **1** (left) and **2** (right). Inset: Schematic crystallographic structure of FeCo Prussian blue analogue. The vacancies at the $[\text{Fe}(\text{CN})_6]$ site are omitted for clarity.

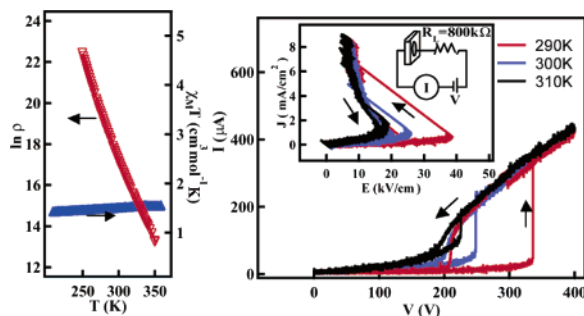


Figure 2. (Left) Temperature dependence of resistivity (red) and magnetization (blue) of compound **3**. (Right) I - V curves of a circuit composed of the FeCo Prussian blue analogue and $R_L = 800$ k Ω in series. Inset: J vs E curves, where $J = I/S$ and $E = (V - IR_L)/d$ (S : cross sectional area, d : distance between the electrodes).

the $\chi_M T$ values for **3** show almost no change (Figure 2), meaning that it does not exhibit a phase transition in the temperature range between 5 and 350 K. An investigation of photoeffects for **1**, **2**, and **3** shows that they exhibit photoinduced magnetization effects. These properties are consistent with those reported previously.⁴

The three samples were subjected to pressed pellet conductivity measurements. These measurements were carried out by a conventional two-terminal method on samples with a typical thickness of 0.25 mm. The applied voltage was always much lower than 1 V. The resistivity vs. temperature (ρ - T) curve for compound **1** shows an abrupt change in conductivity at the temperature where the phase transition between $\text{Fe}^{\text{II}}\text{-LS-CN-Co}^{\text{III}}\text{-LS}$ and $\text{Fe}^{\text{III}}\text{-LS-CN-Co}^{\text{II}}\text{-HS}$ occurs. Furthermore, the figure clearly shows that the ρ - T curve exhibits a hysteresis loop. The activation energy of the electrical conduction for the high-temperature and the low-temperature phases are 0.34 and 0.56 eV, respectively. Similarly,

[†] Kanagawa Academy of Science and Technology.

[‡] Keio University.

the ρ - T curve for compound **2** shows a hysteresis loop at around 225 K. This means that not only magnetic properties but also conductivity can take two different values within the hysteresis loop, allowing the observation of thermally induced conductivity switching over a given temperature range. It should be noted that the temperature where bistability is exhibited can be continuously controlled by varying the Co-to-Fe ratio in the FeCo Prussian blue,^{4b} meaning that the conductance-switching temperature can be tuned by slightly changing the composition, which is distinct from conventional switching materials.

Additional interesting properties were found for compound **3** when the conductivity was measured under higher electric field. The ρ - T curve of **3** measured under electric fields lower than 1 V shows typical semiconducting properties with activation energy equal to 0.68 eV (Figure 2). However, the current-voltage (I - V) plot shows a remarkable nonlinear effect when a higher electric field was applied to it. The I - V characteristics at high voltage were measured for a circuit that included a pellet of **3** as the resistive element and the load resistor ($R_L = 800 \text{ k}\Omega$) in series (Figure 2).⁶ The load resistor was used to avoid a sudden burst of current when the resistance of the sample was changed. Figure 2 shows the I - V characteristics measured at $T = 290, 300,$ and 310 K . The current flowing in the circuit when $T = 300 \text{ K}$ and $V = 100 \text{ V}$ is less than $10 \mu\text{A}$. When the voltage is further increased, the I - V curves apparently became nonlinear. When the voltage reaches $V = 250 \text{ V}$, the current abruptly increases. The current at $V = 300 \text{ V}$ is about $280 \mu\text{A}$, where the applied voltage is partially loaded on the load resistor. These data show that the transition from the high-resistive state to the low-resistive state occurred at 250 V .⁶ The inset in Figure 2 shows the J (current density) vs E (electric field) curves. As the voltage increases, the sample shows a transition from the high-resistive state with a positive differential resistance to the low-resistive state with a negative differential resistance. That is, negative resistance effects were induced in compound **3**.

It has been reported that several charge transfer (CT) complexes such as $\text{TTeC}_1\text{TTF-TCNQ}$ (TTeC_1TTF : tetrakis methyltelluro tetrathiafulvalene, TCNQ : 7,7,8,8-tetracyanoquinodimethane) can exhibit negative resistance effects.⁶ The nonlinear behavior in the FeCo Prussian blue analogues is similar to that of the CT complexes. Because it has been reported that the switching phenomenon has the character of a bulk phase transition induced by an electric field,⁶ the present current switching phenomenon might also be induced by the induction of the $\text{Fe}^{\text{III-Ls}}-\text{CN}-\text{Co}^{\text{II-Hs}}$ sites in the $\text{Fe}^{\text{II-Ls}}-\text{CN}-\text{Co}^{\text{III-Ls}}$ phase. Partial oxidation and reduction of the Fe and Co sites may enhance the conductivity of the compounds. Furthermore, the formation of the $\text{Fe}^{\text{III-Ls}}-\text{CN}-\text{Co}^{\text{II-Hs}}$ sites makes the creation of additional sites easier due to a self-accelerating process,⁸ which may contribute to the abrupt change in conductivity. However, the converted fraction is not so large under conditions where reversible switching is observed. Indeed, we could not detect changes in the IR spectra during the application of the electric field. To acquire a deeper understanding of the conductance-switching phenomenon, a further systematic study is necessary.

It should be noted that one might raise the possibility that the change in the resistance was induced by the electrochemical redox in the solid state. That is, when an external electric field is applied to Prussian blue analogues containing alkali cations in interstitial sites, nonohmic I - V curves resulting from Faradaic current were observed.⁹ However, the reported redox voltage is relatively quite small. For example, the voltages of soluble Prussian blue, $\text{KFe}^{\text{III}}[\text{Fe}^{\text{II}}(\text{CN})_6]$ and CuFe Prussian blue, $\text{K}_{1.1}\text{Cu}_{1.15}[\text{Fe}^{\text{III}}(\text{CN})_6]$ are about

0.83 and 0.53 V, respectively.⁹ These voltages correspond to the differences between the formal potentials of the system's two redox reactions. Hence, the conductance switching effects observed at high-electric field are phenomena different from those reported previously.

In summary, we have shown that FeCo Prussian blue can exhibit conductivity switching by varying the temperature and by applying an electric field. This shows that FeCo Prussian blue is a characteristic multifunctional material with conductivity-switching properties as well as bistability in its magnetic and optical properties.

Acknowledgment. We thank Dr. T. Kawamoto for giving us valuable suggestions. This work was supported by a Grant-in-Aid for Scientific Research on Priority Areas (417) from Ministry of Education, Science, Sport and Culture of Japan.

Supporting Information Available: Temporal response of the current switching, IR spectra of **3** during the application of the electric field, temperature dependence of the resistivity and the magnetization of $\text{Na}_{0.40}\text{Co}^{\text{II}}_{1.30}[\text{Fe}^{\text{III}}(\text{CN})_6] \cdot 5.2\text{H}_2\text{O}$, and other supplementary information. This material is available free of charge via the Internet at <http://pubs.acs.org>

References

- (1) (a) Nakamura, T.; Akutagawa, T.; Honda, K.; Underhill, A. E.; Coomber, A. T.; Friend, R. H. *Nature* **1998**, *394*, 159–162. (b) Coronado, E.; Galn-Mascaros, J. R.; Gomez-Garcia, C. J.; Laukhin, V. *Nature* **2000**, *408*, 447–449. (c) Kurmoo, M.; Graham, A. W.; Day, P.; Coles, S. J.; Hursthouse, M. B.; Caulfield, J. L.; Singleton, J.; Pratt, F. L.; Hayes, W.; Ducasse, L.; Guionneau, P. *J. Am. Chem. Soc.* **1995**, *117*, 12209–12217. (d) Kobayashi, H.; Tomita, H.; Naito, T.; Kobayashi, A.; Sakai, F.; Watanabe, T.; Cassoux, P. *J. Am. Chem. Soc.* **1996**, *118*, 368–377. (e) Itkis, M. E.; Chi, X.; Cordes, A. W.; Haddon, R. C. *Science* **2002**, *296*, 1443–1445.
- (2) Tacconi, N. R.; Rajeshwar, K.; Lezna, R. O. *Chem. Mater.* **2002**, *15*, 3046–3062.
- (3) (a) Ferlay, S.; Mallah, T.; Ouahes, S.; Veillet, P.; Verdagur, M. *Nature* **1995**, *378*, 701–703. (b) Håltveik, F.; Buschmann, W. E.; Zhang, J.; Manson, J. L.; Miller, J. S. *Adv. Mater.* **1999**, *11*, 914–918.
- (4) (a) Sato, O.; Iyoda, T.; Fujishima, A.; Hashimoto, K. *Science* **1996**, *272*, 704–705. (b) Shimamoto, N.; Ohkoshi, S.; Sato, O.; Hashimoto, K. *Inorg. Chem.* **2002**, *41*, 678–684. (c) Varret, F.; Goujon, A.; Bleuzen, A. *Hyperfine Interact.* **2001**, *134*, 69–80. (d) Bleuzen, A.; Lomenech, C.; Escax, V.; Villain, F.; Varret, F.; Moulin, C. C.; Verdaguer, M. *J. Am. Chem. Soc.* **2000**, *122*, 6648–6652. (e) Pejakovic, D. A.; Manson, J. L.; Miller, J. S.; Epstein, A. J. *Phys. Rev. Lett.* **2000**, *85*, 1994–1997. (f) Sato, O.; Einaga, Y.; Iyoda, T.; Fujishima, A.; Hashimoto, K. *Inorg. Chem.* **1999**, *38*, 4405–4412.
- (5) (a) Fielding, D. F.; Mellor, D. P. *J. Chem. Phys.* **1954**, *22*, 1155–1156. (b) Inoue, H.; Yanagisawa, S. *J. Inorg. Nucl. Chem.* **1974**, *36*, 1409–1411.
- (6) (a) Potember, R. S.; Poehler, T. O.; Cowan, D. O. *Apply. Phys. Lett.* **1979**, *34*, 405–407. (b) Kumai, R.; Okimoto, Y.; Tokura, Y. *Science* **1999**, *284*, 1645–1647. (c) Potember, R. S.; Poehler, T. O.; Rappa, A.; Cowan, D. O.; Bloch, A. N. *J. Am. Chem. Soc.* **1980**, *102*, 3659–3660. (d) Tokura, Y.; Okamoto, H.; Koda, T.; Mitani, T.; Saito, G. *Phys. Rev. B* **1988**, *38*, 2215–2218. (e) Iwasa, Y.; Koda, T.; Tokura, Y.; Koshihara, S.; Iwasawa, N.; Saito, G. *Appl. Phys. Lett.* **1989**, *55*, 2111–2113.
- (7) Compound **1** was synthesized by reacting a mixed aqueous solution of $\text{CoCl}_2 \cdot 6\text{H}_2\text{O}$ (2 mmol dm^{-3}) and NaCl (5 mol dm^{-3}) with a mixed aqueous solution of $\text{K}_3\text{Fe}(\text{CN})_6$ (2 mmol dm^{-3}) and NaCl (5 mol dm^{-3}). Anal. Calcd for $\text{Na}_{0.5}\text{Co}^{\text{II}}_{1.25}[\text{Fe}^{\text{III}}(\text{CN})_6] \cdot 4.8\text{H}_2\text{O}$: Na, 3.00; Co, 19.2; Fe, 14.6; C, 18.8; N, 21.9; H, 2.5. Found: Na, 2.98; Co, 19.0; Fe, 14.3; C, 19.7; N, 22.3; H, 2.7. Compound **2** was synthesized by reacting a mixed aqueous solution of $\text{CoCl}_2 \cdot 6\text{H}_2\text{O}$ (2 mmol dm^{-3}) and NaCl (1 mol dm^{-3}) with a mixed aqueous solution of $\text{K}_3\text{Fe}(\text{CN})_6$ (2 mmol dm^{-3}) and NaCl (1 mol dm^{-3}). Anal. Calcd for $\text{Na}_{0.38}\text{Co}^{\text{II}}_{1.31}[\text{Fe}^{\text{III}}(\text{CN})_6] \cdot 5.4\text{H}_2\text{O}$: Na, 2.21; Co, 19.5; Fe, 14.1; C, 18.2; N, 21.3; H, 2.8. Found: Na, 2.26; Co, 19.3; Fe, 14.0; C, 18.8; N, 21.5; H, 2.8. Compound **3** was synthesized by reacting a mixed aqueous solution of $\text{CoCl}_2 \cdot 6\text{H}_2\text{O}$ (2 mmol dm^{-3}) and RbCl (1 mol dm^{-3}) with a mixed aqueous solution of $\text{K}_3\text{Fe}(\text{CN})_6$ (2 mmol dm^{-3}) and RbCl (1 mol dm^{-3}). Anal. Calcd for $\text{Rb}_{0.5}\text{Co}_{1.25}[\text{Fe}(\text{CN})_6] \cdot 5.9\text{H}_2\text{O}$: Rb, 9.8; Co, 16.9; Fe, 12.8; C, 16.6; N, 19.3; H, 2.8. Found: Rb, 10.0; Co, 16.1; Fe, 12.2; C, 17.2; N, 19.9; H, 2.6.
- (8) Hauser, A.; Jetic, J.; Romstedt, H.; Hinek, R.; Spiering, H. *Coord. Chem. Rev.* **1999**, *190–192*, 471–491.
- (9) (a) Kulesza, P. J. *J. Electroanal. Chem.* **1990**, *289*, 103–116. (b) Makowski, O.; Stroka, J.; Kulesza, P. J.; Malik, M. A.; Galus, Z. *J. Electroanal. Chem.* **2002**, *532*, 157–164.

JA06329S